



## Preparation and electrocatalytic dechlorination performance of Pd/Ti electrode

Jingli Zhang<sup>a,\*</sup>, Zhanping Cao<sup>b</sup>, Yongzhi Chi<sup>a</sup>, Liping Xie<sup>b</sup>, Ligang Lin<sup>b</sup>

<sup>a</sup>School of Environmental and Municipal Engineering, Tianjin Chenjian University, Tianjin 300384, China, Tel. +86 22 23085117; email: [jinglizhang2014@tcu.edu.cn](mailto:jinglizhang2014@tcu.edu.cn)

<sup>b</sup>School of Environmental and Chemical Engineering, Tianjin Polytechnic University, Tianjin 300387, China

Received 26 August 2013; Accepted 5 March 2014

### ABSTRACT

The Pd/Ti working electrode was prepared by the electrochemical deposition on the Ti plate and its structure and morphology were analyzed by an X-ray diffraction (XRD) and a transmission electron microscopy. The results showed that Palladium (Pd) crystals were coated uniformly on Titanium (Ti) base material with the average size of 8.69 nm. The cyclic voltammetry was employed to study the electrochemical reduction characteristics of 2,4,5-tripolychlorinated biphenyl (PCB29) in an electrocatalytic system. The results showed that the PCB29 dechlorination was a two-electron transfer reduction controlled by adsorption and conformed to the characteristics of the first-order reaction. The efficiencies of PCB29 degradation in the electrocatalytic system were more than 95% after 5 h at its concentration (mg/L) of 60, 80, and 100. The dechlorinations of PCB29 obeyed the pseudo-first-order reaction kinetic behavior. The reaction rate constant was approximately  $0.011 \text{ min}^{-1}$ . The reaction rate increased slightly as the temperature rose. The 2,5-PCB was first mainly generated by PCB29 para-position dechlorination, 2-PCB by meta-position dechlorination, and then diphenyl by the subsequent ortho-position dechlorination. Diphenyl could be further hydrogenated to phenyl cyclohexane. The chlorine substitution position on PCB29 mainly affected the order of PCB29 electrocatalytic dechlorination.

*Keywords:* Pd/Ti electrode preparation; 2,4,5-tripolychlorinated biphenyl (PCB29); Electrocatalytic dechlorination; Degradation mechanism

### 1. Introduction

Polychlorinated biphenyls (PCBs) are the chemicals formed by attaching one or more chlorine atoms to a pair of connected benzene rings. Depending on the number and position of chlorine atoms attached to the biphenyl ring, 209 different PCB congeners can be formed. PCBs are widely used as raw chemical materials for the production of lubricants and flame

retardants. The chemical and toxicological properties of PCBs vary from one congener to another. PCBs are persistent organic pollutants and difficult to be degraded. The wastewater containing PCBs are refractory, teratogenic, carcinogenic, and mutagenic [1]. The traditional methods for removing PCBs, such as biological method, chemical method, and adsorption process, are slow and incomplete in degrading PCBs and expensive in use [2–4]. In recent years, the electrocatalytic reduction is widely used for dechlorination of

\*Corresponding author.

chlorinated organic pollutants [4]. The hydrogen donors (electrons) are provided by an applied electric field to achieve the PCBs dechlorination and to reduce the PCBs toxicity [5]. In the electrocatalytic reaction, the material of cathode electrode has great influence on PCBs dechlorination efficiency [6]. The good capability of Palladium (Pd) storing and slowly releasing electrons has drawn more and more attention. Titanium was commonly used as an electrode substrate because of its good conductivity, stability, and surface mass transfer performance [7]. Some researchers prepared Pd/Ti electrodes by the electrochemical deposition for the dechlorination of chlorinated organic compounds [7,8]. And some scholars used other substrate materials, such as foam-nickel and glassy carbon modified by Pd [9–12]. In addition, to gain smaller Pd particle sizes and higher particle dispersion, Perini et al treated the glassy carbon as a substrate material [12]. Pd/Ti working electrode, Ti plate modified by Pd element, only works as a catalyst without any loss [13] and provides the catalytic reaction interface. Because of the good capability of Palladium (Pd) storing electrons, that the electron donors sustainably provided by the Pd/Ti cathode could ensure the effective dechlorination of electrocatalytic reduction [7]. In this paper, the preparation and characterization of Pd/Ti electrode were reported, and PCBs electrochemical dechlorination performance on Pd/Ti electrode was studied using 2,4,5-polychlorinated biphenyl (PCB29) with three chlorine substituents in meta, ortho, and para positions as the target pollutant. Our studies could further promote the development of new electrode preparation and electrocatalytic process and open up a new way for efficient degradation of refractory organic matters.

## 2. Materials and methods

### 2.1. Experimental setup and simulated wastewater

PCB29 (analytical grade,  $\geq 99\%$ ) and PdCl<sub>2</sub> (analytical grade,  $\geq 99.5\%$ ), were obtained from Kewei Company of Tianjin University (China). About 60, 80, and 100 mg/L of PCB29 were prepared in phosphate buffer solution (PBS, 10 mmol/L and pH 7.0) using pure water, respectively. The overall size of all the experimental reactors made of plexiglass, was 100 (length)  $\times$  60 (width)  $\times$  100 mm (height). The size of Ti electrode plate, which was bought from Beijing Hengtai Company (China), was 50 (width)  $\times$  80 mm (height) and the parallel-plate distance of the anode and cathode was 70 mm.

### 2.2. Analytical equipments and methods

The composition, the chemical state, and the electronic state of the elements on the Pd/Ti electrode surface were analyzed by an X-ray photoelectron spectrometer (Kratos AXIS Ultra DLD, Japan) employing a monochromated aluminium K $\alpha$  X-ray source ( $h\nu = 1486.6$  eV). The analysis conditions were a voltage of 15 kV and a current of 10 mA. The data were corrected using C 1s (284.45 eV) in the sample as the internal standard and processed by XPSPEAK software.

The X-ray diffraction (XRD) was examined by an X-ray diffractometer (Rigaku D/max 2500 v/pc, Japan). The conditions were a ray source of Cu K $\alpha$ , a wave length ( $\lambda$ ) of 0.154 nm, a tube voltage of 40 kV, a tube current of 100 mA, a scan rate of 8°/min, and a  $2\theta$  scan range of 10°–90°.

The electrochemical characteristics were monitored by CHI 660C electrochemical workstation (Shanghai Chenhua Instrument Company, China) employing a three-electrode system with a saturated calomel reference electrode (SCE), a Pd/Ti plate as the working electrode, and a Ti plate as the auxiliary electrode. A Luggin capillary connected the reference electrode with the simulated wastewater and the tip of the Luggin capillary near the working electrode was open to the test solution for sensing the solution potential.

Surface morphology of Pd/Ti electrode was analyzed by a field-emission scanning electron microscopy (SEM, HITACHI S-4700, Japan).

PCB29 was monitored quantitatively by high-performance liquid chromatography (HPLC, Shimadzu LC-10A, Japan) equipped with a reverse column (Diamonsil ODS, 150  $\times$  4.6 mm, 5  $\mu$ m) and an SPD-10AV UV-vis detector. The ratio of acetonitrile and water was 90:10 (v/v) in the mobile phase, with a flow rate 1.0 mL/min, a column temperature 30°C, and a UV wave length 254 nm.

The intermediate products of PCB29 degradation were monitored by GC 6890-MS 5973N (Agilent Technologies, USA) equipped with a HP-5 chromatographic column (30 m  $\times$  0.25 mm  $\times$  0.25  $\mu$ m). The temperature programming was elevated from an initial temperature of 60°C up to 140°C at a rate of 20°C/min, ramped to 220°C at a rate of 4°C/min, increased to 260°C at a rate of 10°C/min, and then held for 10 min at 260°C. The other analysis conditions were inlet temperature of 260°C, electron ionization mode, ion source temperature of 230°C, and carrier gas flow rate of 1.0 mL/min. The chloride ion content was determined by an ion chromatography (ICS-1500, Dionex Corp., USA) equipped with an IC-A3 column (4.6 mm  $\times$  15 cm) and a non-suppressed conductivity

detector. The analysis conditions were a flow rate of 1 mL/min and a sample volume of 50  $\mu$ L.

### 2.3. Preparation of Pd/Ti working electrode

The electrochemical deposition is an effective method for the material modified by functional metal. The Pd/Ti working electrode, Ti plate modified by Pd element, was prepared by electrochemical deposition. Ti plate was first polished with abrasive paper progressively, put into 0.1 mol/L of sulfuric acid solution for 1 min, rinsed with distilled water, and then placed into the deposition solution which contained (per L) PdCl<sub>2</sub> of 0.16 mol and HCl of 0.1 mol. The electro-deposition of Pd element on Ti plate was carried out by constant potential method, while the platinum plate was used as the counter electrode and a SCE as the reference electrode. The effect of deposition time on the electrode performance was determined under the constant potential of  $-0.25$  V.

## 3. Results and discussion

### 3.1. Effect of deposition time on the Pd deposition of Ti plate

The composition, the chemical, and electronic state of the elements on the Pd/Ti electrode surface were analyzed and the two XPS spectra at the deposition times of 100 and 250 s are shown (Fig. 1). XPS spectra of Pd-3d could be divided into two peaks, Pd (0) and Pd (II). The Pd (0) and Pd (II) binding energies were 335.42 and 340.70 eV at 100 s, respectively. Accordingly, the Pd (0) and Pd (II) binding energies were 335.30 and 340.65 eV at 250 s, respectively. With the deposition time extension, the binding energies of Pd element on Pd/Ti electrode decreased a little, showing that Pd (II) was gradually reduced to Pd (0). With the deposition time extension, the Pd loading amount rose, the mutual effect of electrons between Pd atoms and Ti atoms increased, and the electrocatalytic activity and stability of Pd on the Pd/Ti electrode could be improved [14]. The electrons shifted from Ti atoms to Pd atoms and the peak value of Pd 3d binding energy with catalytic activity on the electrode surface was closer to that of pure Pd. The atomic ratio of Pd and Ti was calculated to be approximately 2:1 by the area integration of the Pd 3d and Ti after subtracting the background from the spectra at the deposition time of 100 s and the atomic ratio of Pd and Ti approximately 4:1 at the deposition time of 250 s. When the deposition time was longer than 250 s, the XPS spectra changed little, showing that the electro-deposition process had been finished. The Pd layer was tightly deposited on the surface of Ti plate

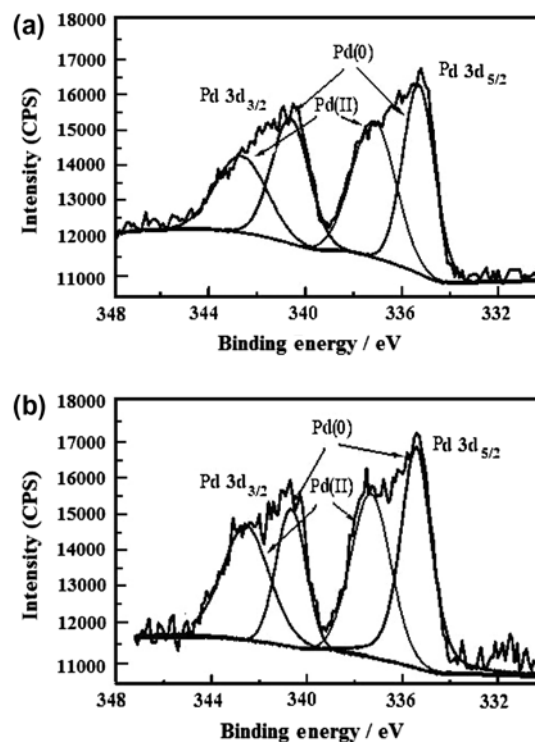


Fig. 1. 3d XPS spectrum of Pd in deposition solution (per L) with PdCl<sub>2</sub> of 0.16 mol and HCl of 0.1 mol under the constant potential of  $-0.25$  V (a) deposition time of 100 s and (b) deposition time of 250 s.

and was not easy to break off. According to the spectrum, the two XPS characteristic peaks (Fig. 1(b)) corresponded to Pd (0) and Pd (II), and the amount of Pd (0) accounted for 64% and that of Pd (II) for 36% in accordance with their area ratio. Therefore, Pd/Ti plate at the deposition time of 250 s was used as the catalytic electrode, and its characterization and catalytic degradation were studied in this experiment.

### 3.2. Structure and characterization of the Pd/Ti electrode

The XRD spectrum and the SEM spectrum of the Pd/Ti plate are seen in Figs. 2 and 3, respectively. Fig. 2 showed that the Pd/Ti electrode prepared in this experiment had obvious diffraction peaks at  $2\theta$  diffraction angles of  $40.519^\circ$ ,  $46.728^\circ$ ,  $68.377^\circ$ ,  $82.332^\circ$ , and  $87.014^\circ$ , corresponding to the Pd crystal face of (1 1 1), (2 0 0), (2 2 0), (2 2 2), and (3 1 1), respectively. This indicated that the Pd metal on Ti plate existed in a face-centered cubic crystal structure [15]. According to Scherrer equation:

$$d = \frac{K\lambda}{\beta \cos \theta} \quad (1)$$

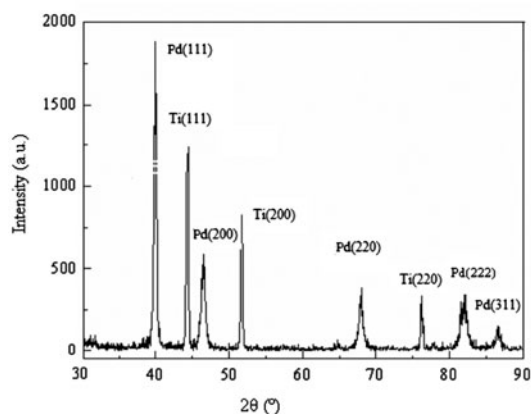


Fig. 2. XRD patterns of Pd/Ti electrode in deposition solution (per L) with  $\text{PdCl}_2$  of 0.16 mol and HCl of 0.1 mol under constant potential of  $-0.25$  V and deposition time of 250 s.

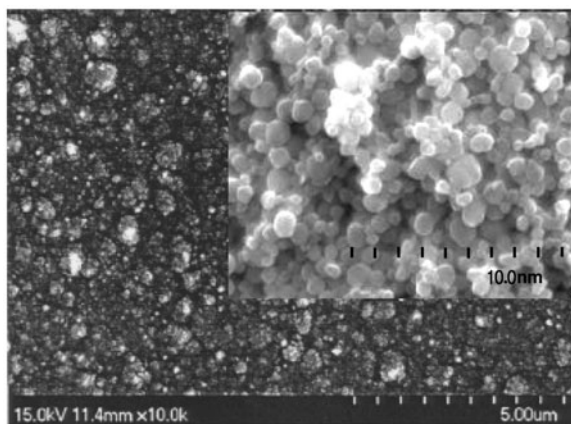


Fig. 3. SEM images of Pd/Ti electrode in deposition solution (per L) with  $\text{PdCl}_2$  of 0.16 mol and HCl of 0.1 mol under constant potential of  $-0.25$  V and deposition time of 250 s (the image at the upper right corner with greater magnification).

where  $d$  (nm) is the mean particle size,  $K$  is a dimensionless shape factor and its typical value is 0.9,  $\lambda$  is the X-ray wavelength (0.154 nm),  $\beta$  (radian) is the half peak width at the maximum intensity after subtracting the instrumental line, and  $\theta$  (radian) is the Bragg angle to which the crystal plane of the strongest diffraction peak corresponds. According to Pd(111), the crystal face  $2\theta$  was  $39.8^\circ$  and  $2\beta$  was  $1.94^\circ$ , the average size of Pd crystals in the catalyst was calculated to be 8.69 nm, which indicated that Pd(0) had been successfully deposited on the electrode surface.

The treated surface of Ti plate was conducive to the deposition and dispersal of Pd metal element. The

black crystals (Fig. 3) were uniformly distributed on the surface of Ti plate and had obvious spatial extension. This distribution helps to increase the number of the catalytic active sites and to improve the utilization rate of Pd catalyst [16]. The average crystal size was 9.6 nm (Fig. 3) and the value was close to the result of the above calculation using the Scherrer equation.

### 3.3. Electrochemical performance of the Pd/Ti electrode

Fig. 4 showed the cyclic voltammograms (CV) of the Pd/Ti electrode in the phosphate buffered solution (pH 7.0) without PCB29 and with PCB29 of 80 mg/L at the various scan rates (every scan rate for five cycles). When the potential ranged from 0 to  $-1.5$  V (vs. SCE), there were two oxidation-reduction peaks at  $-0.72$  and  $-0.84$  V (vs. SCE) in the solution with PCB29 of 80 mg/L and the peak potential difference ( $\Delta E_p$ ) was 0.12 V, which showed the good electron transfer performance and the reversibility of the electrode surface. When the scan rate ranged from 50 to 250 mV/s, the peak current rose with the increase of the scan rate (Fig. 5).

With the increase of the scan rate, the peak potentials on the anode showed a small offset in positive direction and the peak potentials on the cathode also showed a small offset in negative direction. Therefore the  $\Delta E_p$  value increased. There was a positive linear relationship between the peak value of the oxidation current and the scan rate, while there was a negative linear relationship between the peak value of the reduction current and the scan rate. The ratio of the two values was close to 1 at the same scan rate.

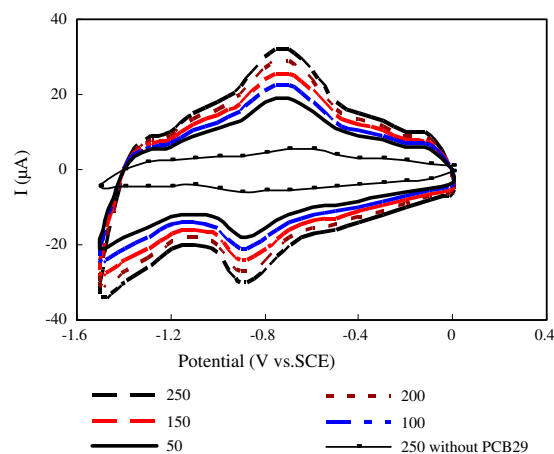


Fig. 4. CV of the Pd/Ti electrode at various scan rates  $v$  (mV/s) in the phosphate buffered solution (pH 7.0) with PCB29 of 80 mg/L or without PCB29 under the potential range from 0 to  $-1.5$  V (vs. SCE).

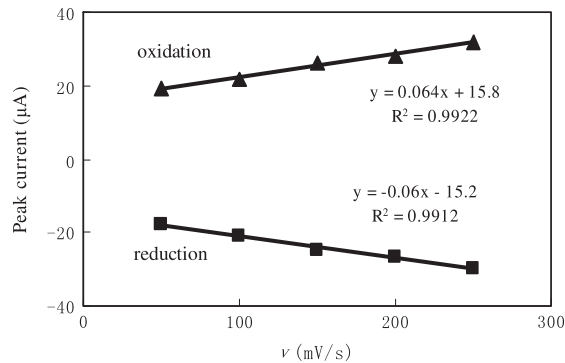


Fig. 5. Linear relationship of the peak currents and scan rate in the phosphate-buffered solution (pH 7.0) with PCB29 of 80 mg/L under the potential range from 0 to  $-1.5$  V (vs. SCE).

The PCB29 diffusion in the solution was not the control step for the electrocatalytic reaction of PCB29 dechlorination. The reduction was carried out due to the reaction of PCB29 with active hydrogen stored on the electrode surface. The process was a direct electrochemical reduction [17–19], which could be explained by further electrode reaction controlled by adsorption process within the scan rate range [20,21]. Laviron equation [22] is used for the quantitative relationship of the reaction which is not controlled by diffusion in the solution. Laviron equation is,

$$I_p = \frac{nFQv}{4RT} \quad (2)$$

where  $I_p$  (A) is the reduction current peak,  $n$  (mol) is the number of electrons per reaction mol,  $F$  is Faraday's constant,  $Q$  (Coulomb, C) is the quantity of electric charge which is calculated by the reduction peak integration,  $v$  (mV/s) is the scan rate,  $R$  is the molar gas constant, and  $T$  (K) is the absolute thermodynamic temperature. By calculating Eq. (2)  $n$  was 2.054 in the electrocatalytic system, which showed that the PCB29 dechlorination was a two-electron transfer reaction. PCB29 accepted an electron and simultaneously lost one chloride ion.

#### 3.4. Degradation kinetics of PCB29 electrocatalytic reduction

The dynamic characteristics of the PCB29 electrocatalytic degradation were compared at various initial concentrations (Fig. 6). The experimental conditions were at a temperature of  $20^\circ\text{C}$  and an applied potential of  $-0.84$  V (vs. SCE). The PCB29 concentrations

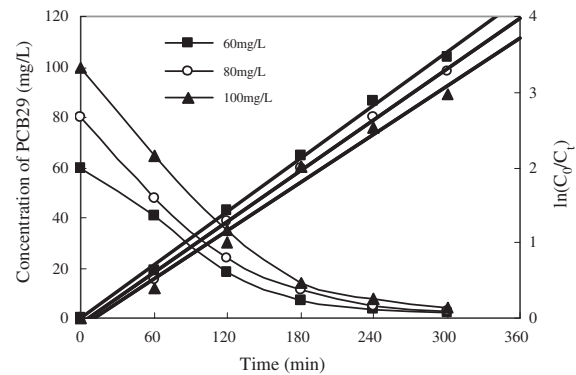


Fig. 6. Characteristic diagram of PCB29 electrical catalytic degradation at different concentrations under a temperature of  $20^\circ\text{C}$  and an applied potential of  $-0.84$  V.

were 60, 80, and 100 mg/L, respectively. The PCB29 degradation efficiency is calculated as,

$$\eta = \frac{C_0 - C_t}{C_0} \times 100\% \quad (3)$$

where  $\eta$  is the degradation efficiency,  $C_0$  (mg/L) is the initial concentration, and  $C_t$  (mg/L) is the concentration at time  $t$ .

The efficiencies of PCB29 degradation in the electrocatalytic system were more than 95% after 5 h. When the initial content of PCB29 increased from 60 to 100 mg/L, the degradation rate was faster. It was speculated that more Pd activation sites of the Pd/Ti electrode were involved in reductive degradation with the increase of the PCB29 content. The Pd/Ti electrode has good hydrogen-storage properties [23] and can utilize hydrogens to dechlorinate the pollutant better. The adsorption capacity of the electrode surface and the potential activation of the reaction interface are favorable for the dehalogenation [24], and thus the high efficient degradation is easily achieved.

The dynamics equations of PCB29 degradation were gained by fitting the experimental data (Fig. 7). Dechlorination reactions at three concentrations of PCB29, which obeyed the pseudo-first-order reaction kinetic behavior. The reaction rate constant was approximately  $0.011 \text{ min}^{-1}$  and changed a little. The correlation coefficient  $R$  was greater than 0.98.

#### 3.5. Effect of reaction temperature on the PCB29 dechlorination

The temperature generally affects the electrode reaction and the chemical process. S. Arrhenius equation was employed to analyze the effect of

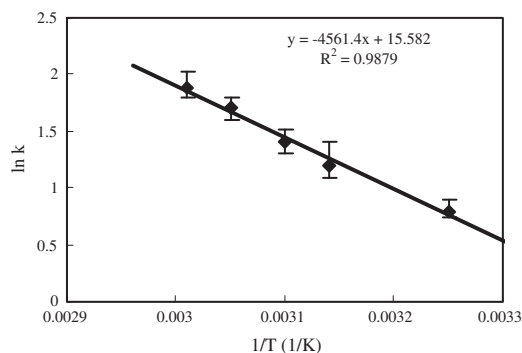


Fig. 7. Effect of temperature on PCB29 electrical catalytic degradation with the initial PCB29 concentration of 80 mg/L.

temperature on the electrocatalytic reduction of PCB29 at the Pd/Ti electrode and this equation is,

$$\ln k = -\frac{Ea}{R} \cdot \frac{1}{T} + \ln A = -a \cdot x + b \quad (4)$$

where  $k$  (1/h) is the overall reaction rate constant,  $A$  is the pre-exponential factor,  $Ea$  (J/mol) is the activation energy,  $R$  (8.314 J/molK) is the gas constant, and  $T$  (K) is the absolute temperature. The rate of the PCB29 dechlorination was positively associated with the increase of the reaction temperature when the initial concentration was 80 mg/L (Fig. 8). The natural (base e) logarithm of the PCB29 reductive dechlorination rate constants showed a negative linear relationship ( $R^2=0.988$ ) with the reciprocal of the absolute temperature. The activation energy for PCB29 dechlorination was calculated to be 37.9 kJ/mol by Eq. (4) in the electrocatalytic system and the surface reduction of PCB29 dechlorination involved the transfer of two electrons. The typical values of activation energy ( $Ea$ ) for transport-controlled reactions range from 8 to 25 kJ/mol [25]. The activation energy of the PCB29 dechlorination on the Pd/Ti electrode was 37.9 kJ/mol, so the dechlorination was not limited by the mass transfer process but mainly by the surface adsorption. Because the activation energy is much lower than that of most chemical reactions (60–250 kJ/mol), the dechlorination reaction happened easily. The activation energy was small and positive, showing that the reaction rate increased slightly as the temperature rose, but was not sensitive to the temperature. The reaction controlled by the adsorption is not as sensitive as that controlled by the chemical process.

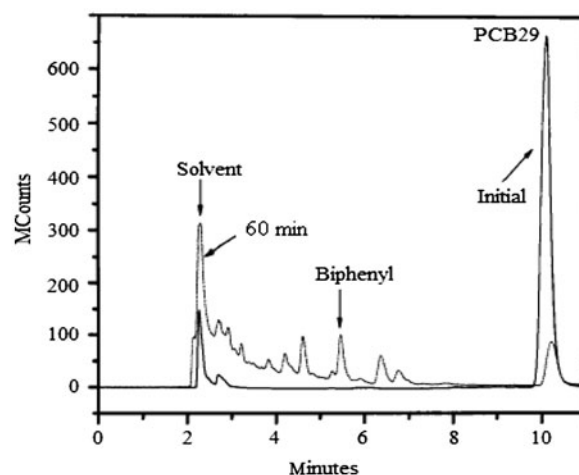


Fig. 8. Liquid chromatography spectrogram of initial PCB29 sample with PCB29 of 80 mg/L and electrocatalytic reduction at 60 min.

### 3.6. Analysis of electrocatalytic degradation of PCB29

The HPLC spectrogram at the reaction time of 60 min was compared with that of the initial concentration of 80 mg/L (Fig. 8). There were only the solvent peak and the PCB29 peak at the beginning. There appeared series of new product peaks at the reaction time of 60 min and the PCB29 peak area decreased obviously. The GC-MS analysis of these products is seen in Fig. 9. Comparison with the retention times of the standard spectra, monochlorobiphenyl, dichlorobiphenyl, and phenylbenzene were determined to be the intermediate products in the PCB29 degradation

The concentrations of PCB29 and its intermediate products were quantitatively detected using HPLC at the various reaction times in the electrocatalytic system (Fig. 10).

The first intermediate of PCB29 dechlorination was mainly 2,5-PCB, its concentration increased to the maximum value of 21 mg/L at the reaction time of 90 min, and then reduced slowly. The 2,5-PCB was barely detectable after 300 min. The chlorine at para-position on the benzene ring is unstable due to  $p-\pi$  conjugation of benzene ring [26,27], while the dechlorination of chlorine substituent at ortho-position is blocked because of the electric field induction and the sterically hindered effect of benzene ring. The first product of PCB29 dechlorination was mainly 2,5-PCB and the subsequent was 2-PCB. The change trend of 2-PCB concentration was the same as 2,5-PCB. With the hydrogenation and dechlorination, a small amount of biphenyl could be further hydrogenated to phenyl cyclohexane, and it was concluded that the benzene ring could be opened in the electrocatalytic system.

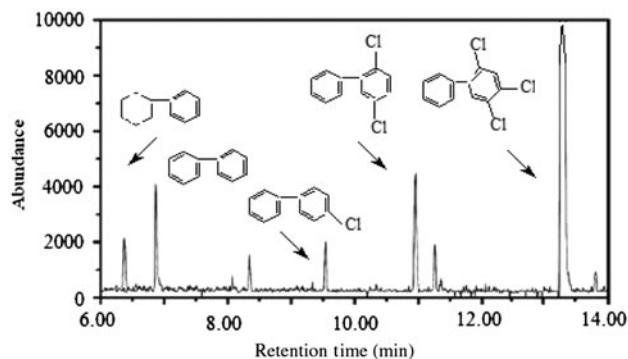


Fig. 9. GC-MS spectrograms in the electrocatalytic reduction at 60 min with the initial PCB29 concentration of 80 mg/L.

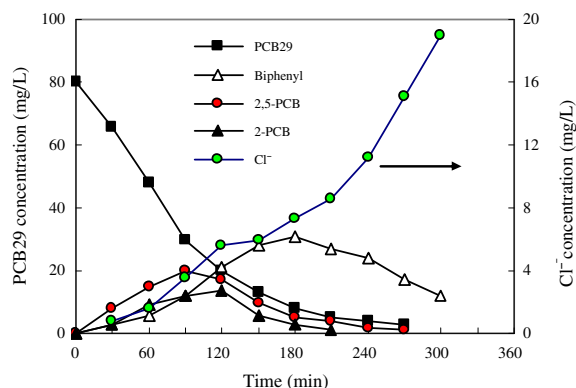


Fig. 10. Concentration variation of substances in PCB29 electrocatalytic reduction with the initial PCB29 concentration of 80 mg/L.

The above results showed that the chloride substitution position of PCB29 molecule played the major role for the difficulty of PCB29 dechlorination. The chloride ion concentration increased with the decrease of PCB29 initial content in the solution. Through the material balance calculation, the amount of chloride ion produced by the PCB29 dechlorination was equal to its increment in the reactor.

#### 4. Conclusions

(1) The Pd nanocrystals were uniformly distributed on Ti plate surface by the electrodeposition method and Pd/Ti working electrode showed the strong reductive ability for PCB29 dechlorination with the degradation efficiency of more than 95%. The electron transfer process was controlled by the adsorption process in the electrocatalytic

system and the PCB29 dechlorination was a two-electron transfer reaction.

- (2) The efficiencies of PCB29 degradation in the electrocatalytic system were more than 95% after 5 h. The dechlorination reactions of PCB29 obeyed the pseudo-first-order reaction kinetic behavior. The reaction rate constant was approximately  $0.011 \text{ min}^{-1}$  and changed a little. The reaction rate increased slightly as the temperature rose, but was not sensitive to the temperature.
- (3) The main pathway of PCB29 degradation in the electrocatalytic system probably was  $\text{PCB29} \rightarrow 2,5\text{-PCB} \rightarrow 2\text{-PCB} \rightarrow \text{biphenyl}$  and phenylbenzene was further hydrogenated to phenyl cyclohexane. The chloride substitution position of PCB29 molecule played the major role for the difficulty of PCB29 dechlorination.

#### Acknowledgments

This work was supported by the National Natural Science Foundation of China (No. 51078265) and Ministry of Housing and Urban-Rural Development of China (No. 2012-K7-20).

#### References

- [1] H. Gomes, C.D. Ferreira, A.B. Ribeiro, Overview of *in situ* and *ex situ* remediation technologies for PCB-contaminated soils and sediments and obstacles for full-scale application, *Sci. Total Environ.* 445–446 (2013) 237–260.
- [2] Z.M. Xiu, Z.H. Jin, T.L. Li, S. Mahendra, G.V. Lowry, P.J.J. Alvarez, Effects of nano-scale zero-valent iron particles on a mixed culture dechlorinating trichloroethylene, *Bioresour. Technol.* 101 (2010) 1141–1146.
- [3] N.S. Babu, N. Lingaiah, P.S.S. Prasad, Characterization and reactivity of  $\text{Al}_2\text{O}_3$  supported Pd-Ni bimetallic catalysts for hydrodechlorination of chlorobenzene, *Appl. Catal. B* 111–112 (2012) 309–316.
- [4] Y.H. Shih, C.Y. Hsu, Y.F. Su, Reduction of hexachlorobenzene by nanoscale zero-valent iron: Kinetics, pH effect, and degradation mechanism, *Sep. Purif. Technol.* 76 (2011) 268–274.
- [5] B. Yang, G. Yu, Z.L. Zhang, Study on the application of electrochemical methods to the destruction of chlorinated aromatic pollutants, *Prog. Chem.* 18 (2006) 87–92.
- [6] B. Yang, G. Yu, D.M. Shuai, Electrocatalytic hydrodechlorination of 4-chlorobiphenyl in aqueous solution using palladized nickel foam cathode, *Chemosphere* 67 (2007) 1361–1367.
- [7] B. Yang, G. Yu, J. Huang, Electrocatalytic reductive dechlorination of 2,4,5-PCB in aqueous solution by palladium-modified Titanium mesh as the cathode, *Acta Phys. Chim. Sin.* 22 (2006) 306–311.

- [8] Z. Sun, H. Ge, X. Hu, Y. Peng, Electrocatalytic dechlorination of chloroform in aqueous solution on palladium/Titanium electrode, *Chem. Eng. Technol.* 32 (2009) 134–139.
- [9] Z.Q. He, K.J. Lin, J.J. Sun, L.N. Wen, C. Gao, J.M. Chen, S. Song, Y.Y. Qian, W.P. Liu, Kinetics of electrochemical dechlorination of 2-chlorobiphenyl on a palladium-modified nickel foam cathode in a basic medium: From batch to continuous reactor operation, *Electrochim. Acta* 109 (2013) 502–511.
- [10] Z.R. Sun, B.H. Li, X. Hu, M. Shi, Q.N. Hou, Y.Z. Peng, Electrochemical dechlorination of chloroform in neutral aqueous solution on palladium/foam-nickel and palladium/polymeric pyrrole film/foam-nickel electrodes, *J. Environ. Sci.* 20 (2008) 268–272.
- [11] I.G. Casella, M. Contursi, Electrocatalytic reduction of chlorophenoxy acids at palladium-modified glassy carbon electrodes, *Electrochim. Acta* 52 (2007) 7028–7034.
- [12] L. Perini, C. Durante, M. Favaro, S. Agnoli, G. Granozzi, A. Gennaro, Electrocatalysis at palladium nanoparticles: Effect of the support nitrogen doping on the catalytic activation of carbon-halogen bond, *Appl. Catal., B* 144 (2014) 300–307.
- [13] J.P. Liu, J.Q. Ye, C.W. Xu, S.P. Jiang, Y.X. Tong, Kinetics of ethanol electrooxidation at Pd electrodeposited on Ti, *Electrochem. Commun.* 9 (2007) 2334–2339.
- [14] S.J. Bae, K.S. Nahm, P. Kim, Electroreduction of oxygen on Pd catalysts supported on Ti-modified carbon, *Curr. Appl. Phys.* 12 (2012) 1476–1480.
- [15] Y.C. Zhao, L. Zhan, J.N. Tian, S.L. Nie, Z. Ning, N-doped amorphous carbon supported Pd catalysts for methanol electrocatalytic oxidation, *Acta Phys. Chim. Sin.* 27 (2011) 91–96.
- [16] M.C. Li, N.N. You, C.A. Ma, Studies on electrochemical dechlorination reaction of 3-chlorobenzoic acid on Pd/Ti electrode, *Acta Chim. Sin.* 69 (2011) 2762–2766.
- [17] M.S. Liang, Y. Bai, M. Liu, W.J. Zheng, Electrochemical reaction of Cytochrome c at selenocystine self-assembled monolayers modified electrodes, *Acta Phys. Chim.* 25 (2009) 457–462.
- [18] Z.H. Yu, T.T. Su, C.H. Ren, F. Li, D.G. Xia, S.Y. Cheng, Direct electrochemistry and immobilization of glucose oxidase on nano-carbon aerogels, *Acta Phys. Chim. Sin.* 28 (2012) 2867–2873.
- [19] N.D. Zhou, Y. Cao, G.X. Li, Electron transfer and interfacial behavior of redox proteins, *Sci. Chin. Chem.* 53 (2010) 720–736.
- [20] Y.H. Qin, L.H. Zhou, S.T. Wang, H.D. Xu, J.H. Li, Direct electrochemistry of Cytochrome c at nanoporous alumina templates modified electrodes, *Chem. J. Chin. U.* 25 (2004) 636–637.
- [21] X.H. Chen, Studies on the Mechanisms of Proton and Electron Transport and their Modulations in Biological Molecules, Shandong University, Jinan City, 2009.
- [22] E. Laviron, The use of linear potential sweep voltammetry and of a.c. voltammetry for the study of the surface electrochemical reaction of strongly adsorbed systems and of redox modified electrodes, *J. Electroanal. Chem. Interfacial Electrochem.* 100 (1979) 263–270.
- [23] B. Yang, G. Yu, D.M. Shuai, Electrocatalytic hydrodechlorination of 4-chlorobiphenyl in aqueous solution using palladized nickel foam cathode, *Chemosphere* 67 (2007) 1361–1367.
- [24] S. Mentus, A.A. Rabi, D. Jašin, Oxygen reduction on potentiodynamically formed Pd/TiO<sub>2</sub> composite electrodes, *Electrochim. Acta* 69 (2012) 174–180.
- [25] S. Glasstone, K.J. Laidler, H. Eyring, *The Theory of Rate Processes*, McGraw-Hill, New York, NY, 1942.
- [26] J.X. Fu, *Organic Chemistry*, Higher Education Press, Beijing, 2001.
- [27] Z.P. Cao, J.L. Zhang, H.W. Zhang, Electron transfer mechanism of pentachlorophenol (PCP) reduction in power-assisted microbial system, *J. Chem. Ind. Eng. Soc. Chin.* 63 (2012) 4042–4047.